

Insulator Boundary Layers in Magnetohydrodynamic Channels

FRANCIS J. HALE*

U. S. Air Force Academy, Colorado Springs, Colo.

AND

JACK L. KERREBROCK†

Massachusetts Institute of Technology, Cambridge, Mass.

The laminar, compressible boundary layer on the insulating walls of an MHD channel is studied for cases of equilibrium conductivity at the local gas temperature and of equilibrium at the local electron temperature. It is found that the increase in friction and heat transfer due to electromagnetic effects is appreciable for the former case and very large for the latter case, for which a typical Nusselt number is about 10 times that for a normal flat-plate boundary layer.

Introduction

WE shall be concerned in this paper with the behavior of the boundary layers on the insulating walls of a direct-current plasma accelerator. In particular, estimates of the influence of the electromagnetic interaction on friction and heat transfer are desired.

Important effects on these quantities are to be expected in the insulator boundary layer, as in the electrode boundary layer,¹ because it occurs in a flow with very strong external energy coupling, where the rate of energy addition to the fluid depends not only on the fluid mechanical variables but also on the electromagnetic fields. In this respect, electrode and insulator boundary layers in plasma accelerators and magnetogasdynamic generators are quite different from ordinary boundary layers on the external surfaces of bodies. To expand on this point, we note that in a nonconducting gas of Prandtl number unity the boundary layer on an insulated surface has uniform total enthalpy. The same is true in an electrically conducting gas, provided that the current loops close entirely within the gas or, in other words, provided that the electric field is zero.

On the other hand, in insulator and electrode boundary layers, the rate of energy addition to or removal from the fluid in the boundary layer can be quite different from that in the main flow, with the result that the total enthalpy in the boundary layer may also be quite different from that in the main flow, and the heat transfer and skin friction may be greatly altered.

In the insulator boundary layer, this is clearly seen in a phenomenon sometimes referred to as "short circuiting." Part of the voltage applied to the electrodes of a plasma accelerator is offset by the "reverse electromotive force" resulting from fluid motion through the magnetic field, and part is absorbed by resistive drop in the gas. In the boundary layer the reversed electromotive force is smaller, and, if the reduction in the conductivity does not offset this effect, a larger current density will flow there. There is a correspondingly large rate of energy addition in the boundary layer.

This phenomenon has been considered previously by Fay² for an asymptotic boundary layer in incompressible flow of constant conductivity and by Moffatt³ for both laminar and turbulent incompressible flows with a step-varied conductivity. The contribution of the present work is to relax the assumptions of incompressibility and constant conductivity.

The assumption of incompressibility must be relaxed because of the importance of the fluid density to the energy coupling. Since the electromagnetic forces are volumetric forces, the fluid tends to be very strongly influenced by them in regions of low density.

The variation of the conductivity across the boundary layer is clearly of crucial importance, since it, together with the velocity variation, determines the variation of the current density and hence the energy coupling. We shall consider two limiting types of behavior of the conductivity. In the first case, an equilibrium conductivity at the local temperature and pressure is assumed. Such behavior is representative of seeded combustion gases or of seeded air. In the second case, a two-temperature model is adopted for the plasma, as proposed by Kerrebrock.⁴ In this model, the conductivity is strongly coupled to the current density or to the electric field measured in the moving fluid. This greatly complicates the coupling alluded to previously.

The effects of a nonzero Hall parameter (tensor conductivity) will be included. The axial currents due to the presence of a Hall potential in the boundary layer induce a cross flow, rendering the boundary layer three-dimensional.

Only laminar boundary layers will be considered. Similar solutions will be sought, and, in those situations where none can be found, local similarity will be assumed. We shall find for the insulator boundary layer, as for the electrode boundary layer, that similarity exists only for constant freestream temperature and low Mach numbers.

In defense of these two rather gross approximations, we note that our intent is to study the new phenomena that arise due to compressibility and variable conductivity. These are likely to be similar for both laminar and turbulent boundary layers, and, because they are very strong effects, they should not be too sensitive to the approximation of local similarity.

Principal Variations Across the Boundary Layer

The flow channel, magnetic field, and current are shown schematically in Fig. 1, together with the coordinate system that will be used. It will be assumed that the magnetic and electric fields are prescribed, that the electric field is constant in z , and that the magnetic field is constant in y and z . The electric field will, of course, be determined by the

Presented as Preprint 63 201 at the AIAA Summer Meeting, Los Angeles, Calif., June 17-20, 1963; revision received December 6, 1963. This paper is based on the doctoral thesis of the first author accomplished at the Massachusetts Institute of Technology under the sponsorship of the Air Force Institute of Technology. Numerical solutions were obtained by the Computation Center of Massachusetts Institute of Technology.

* Colonel, U. S. Air Force; also Professor and Head of Department of Astronautics. Member AIAA.

† Associate Professor of Aeronautics and Astronautics. Member AIAA.

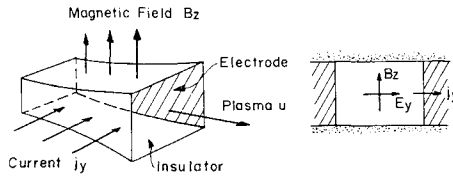


Fig 1 Schematic diagram of the flow channel, showing electrodes and insulators

voltage difference and spacing of the electrodes. The magnetic field would be determined by the distribution of current flow in the gas and in coils external to the channel or by the contours of iron pole pieces. We shall assume that it does not explicitly depend on the currents flowing in the gas, and we shall delete Ampere's law from consideration. This does not mean that Ampere's law is not satisfied, but rather that the magnetic field induced by currents flowing in the gas plus that due to external currents equals the prescribed field.

Current Density Ratios

With the electric and magnetic fields given, the vector current density is determined by a generalized Ohm's law of the form^{5,6}

$$\mathbf{j} = \sigma[\mathbf{E} + (\mathbf{V} \times \mathbf{B}) - (1/ne)(\mathbf{j} \times \mathbf{B})] \quad (1)$$

where σ is the scalar electrical conductivity. The first two terms within the brackets represent the effective electric field with respect to the moving gas, and the third term represents the effective electric field due to motion of the electrons relative to the gas (Hall effect). Ion slip effects have been neglected; the analysis is, therefore, applicable only to slightly ionized gases.

The freestream Hall parameter b_∞ is defined by

$$b_\infty = \omega \tau_e = \sigma_\infty B / n_{e\infty} e \quad (2)$$

If an axial electric field is applied such that $E_x = b_\infty(E_y - u_\infty B)$, then j_∞ , the freestream Hall current, is suppressed. The absence of a transverse Lorentz force $j_x B$ results in $v_\infty = 0$, and the freestream remains one-dimensional. The transverse current in the freestream is then

$$j_\infty = \sigma_\infty(E_y - u_\infty B) \quad (3)$$

Although an appropriate axial field can suppress the Hall current in the freestream, there is still a j_x in the boundary layer, since u , σ , and b vary across the boundary layer. The resulting Lorentz force, $j_x B$, produces a transverse velocity component v .

If we now define the usual electromagnetic loading factor K for the freestream as $K = E_y / u_\infty B$ and refer j_x and j_y to j_∞ , we find

$$\frac{j_x}{j_\infty} = \frac{\sigma}{\sigma_\infty} \left(\frac{1}{1+b^2} \right) \left[b_\infty - \left(\frac{K}{K-1} \right) \times \right. \\ \left. b + \left(\frac{1}{K-1} \right) \left(b \frac{u}{u_\infty} + \frac{v}{u_\infty} \right) \right] \quad (4)$$

$$\frac{j_y}{j_\infty} = \frac{\sigma}{\sigma_\infty} \left(\frac{1}{1+b^2} \right) \left[\left(\frac{K}{K-1} \right) + b b_\infty - \right. \\ \left. \left(\frac{1}{K-1} \right) \left(\frac{u}{u_\infty} - b \frac{v}{u_\infty} \right) \right] \quad (5)$$

These equations show the dependence of the current densities on the nondimensional boundary-layer velocities and on the freestream electromagnetic loading. They also show very clearly the importance of adequately describing the variations of both the electrical conductivity and the Hall parameter across the boundary layer. The expressions used

to describe these variations are so vital to this analysis that they will be discussed at length in the next section.

Electrical Conductivity

In a plasma with a small amount of ionization, such that Coulomb cross sections are negligible compared to neutral-particle cross sections, the electrical conductivity is appropriately represented as

$$\sigma = e^2 n / m_e \nu \quad (6)$$

where n is the electron concentration and ν is the electronic collision frequency.

As was mentioned in the Introduction, we shall consider two limiting cases of the behavior of σ . The first, to be termed the "equilibrium" case, is appropriate in situations where n_e is determined by ionization equilibrium at the local gas pressure and temperature, and the conductivity is determined by electron-atom collisions. Under these conditions, a good representation for the conductivity is¹

$$\sigma / \sigma_\infty = e^{-\lambda[(1/\theta) - 1]} \quad (7)$$

where $\theta = T_e / T_{g\infty}$ and $\lambda = I / 2kT_g$.

The second case, to be termed the "nonequilibrium" case, is that in which the energy coupling between electrons and atoms is very weak, so that the resistive heating of the electrons causes their temperature to rise considerably above that of the gas. Kerrebrock⁴ has proposed that, at sufficiently high electron concentrations, ionization equilibrium may again be assumed, provided that it is evaluated at the electron temperature rather than at the gas temperature. It then follows that the conductivity can be represented as a function of the gas temperature and pressure and of the current density. In the present work, we shall express the electrical conductivity by

$$\sigma / \sigma_\infty = \exp[-\Phi(1-\theta)](j_T/j_\infty)\alpha \quad (8)$$

where α and Φ are constants. The value of α is about 0.8 if the electron temperature is greater than 1.1 times the gas temperature, and Φ is about 3 for a mixture of argon and potassium at 1 atm pressure and 3000°K. The total current density in the boundary layer, j_T , is given by

$$j_T = [j_x^2 + j_y^2]^{1/2} \quad (9)$$

Equation (8) is not yet in final form, since the ratio of current densities is a function of σ / σ_∞ . Substituting Eqs (4) and (5) for j_x and j_y gives the final expression for the electrical conductivity in the case of nonequilibrium ionization:

$$\frac{\sigma}{\sigma_\infty} = \left\{ \exp \left[- \left(\frac{\Phi}{1-\alpha} \right) (1-\theta) \right] \right\} \times \\ \left[\left(\frac{1}{1+b^2} \right) \left[\left(\frac{K}{K-1} \right)^2 + b_\infty^2 - \left(\frac{2}{K-1} \right) \left\{ \left(\frac{K}{K-1} \right) \times \right. \right. \right. \right. \\ \left. \left. \left. \frac{u}{u_\infty} - b_\infty \frac{v}{u_\infty} \right\} + \left(\frac{1}{K-1} \right)^2 \left\{ \left(\frac{u}{u_\infty} \right)^2 + \left(\frac{v}{u_\infty} \right)^2 \right\} \right] \right]^{1/2(1-\alpha)} \quad (10)$$

This expression indicates the complex interactions of the electrical conductivity with the other flow parameters in the presence of electron heating. The exponential factor represents the effect of gas temperature on the conductivity. For a typical gas, as just described, the factor $\Phi/(1-\alpha)$ is about 10, as is the factor λ of Eq (7), so that the sensitivity of σ to the gas temperature is about the same in the case of electron heating as in the equilibrium case. However, in the nonequilibrium case σ is also very sensitive to the magnitude of the electric field, as represented by the second factor in Eq (10). It will be seen later that this coupling can lead to very unusual boundary-layer behavior.

Hall Parameter

Since B is assumed constant, $b \propto 1/\nu \propto T_g/(T)^{1/2}$. For the thermal equilibrium case with the freestream as the reference, the variation of the Hall parameter across the boundary layer becomes simply

$$b/b_\infty = \theta^{1/2} \quad (11)$$

Similarly, for the nonequilibrium case, the Hall parameter in the boundary layer referred to that in the freestream is given by $b/b_\infty = \theta(T_\infty/T)^{1/2}$. Expressing T/T_∞ in terms of j_T/j_∞ , we find $b/b_\infty = \theta(j_T/j_\infty)^\xi$, where ξ is of the order of 0.05. Therefore, the variation with current density will be neglected, leaving

$$b/b_\infty = \theta \quad (12)$$

for the nonequilibrium condition

To a first approximation, the variation of the Hall parameter across the boundary layers is a function only of the gas temperature, regardless of the state of equilibrium. The variation is quite small compared with that of the electrical conductivity, and thermal nonequilibrium increases the sensitivity of the Hall parameter to gas temperature variations.

Boundary-Layer Equations

It was noted previously that the Hall effect renders the insulator boundary layer three-dimensional, since the Lorentz force due to the axial current, $j_z B$, induces a cross flow in the y direction. In general, we should then consider the development of this flow in the y direction as well as the development in the x direction. However, we shall assume uniformity in the y direction. This is equivalent to assuming that the insulators are of infinite extent in y , so that the cross-flow boundary layer has attained its asymptotic form. Actually, of course, it is only necessary that the insulator be several boundary-layer thicknesses wide in order that the approximation be valid.

With this assumption, the boundary-layer equations are as follows:

Continuity

$$\frac{\partial}{\partial x}(\rho u) + \frac{\partial}{\partial z}(\rho w) = 0 \quad (13)$$

Axial Momentum

$$\rho \left(u \frac{\partial u}{\partial x} + w \frac{\partial u}{\partial z} \right) = -\frac{dp}{dx} + \frac{\partial}{\partial z} \left(\mu \frac{\partial u}{\partial z} \right) + j_y B \quad (14)$$

Transverse Momentum

$$\rho \left(u \frac{\partial v}{\partial x} + w \frac{\partial v}{\partial z} \right) = \frac{\partial}{\partial z} \left(\mu \frac{\partial v}{\partial z} \right) - j_z B \quad (15)$$

Energy

$$\rho \left(u \frac{\partial H}{\partial x} + w \frac{\partial H}{\partial z} \right) = \frac{1}{Pr} \frac{\partial}{\partial z} \left(\mu \frac{\partial H}{\partial z} \right) + \left(1 - \frac{1}{Pr} \right) \frac{\partial}{\partial z} \left[\mu \frac{\partial}{\partial z} \left(\frac{u^2 + v^2}{2} \right) \right] + j_x E_x + j_y E_y \quad (16)$$

where H , the total enthalpy, is $H = C_p T + (u^2 + v^2)/2$. We shall assume that the plasma is a perfect gas (so that $p = \rho R T$), that μ is proportional to T , and that C_p and Pr are constants.

The boundary conditions are that at the wall ($z = 0$) $u = v = w = 0$ and $H = H_w$ and at the edge of the boundary layer ($z \rightarrow \infty$) $u = u_\infty$, $v = 0$, and $H = H_\infty$.

The electromagnetic fields introduce a body force into each of the momentum equations and additional terms into the energy equation. The latter represent the total energy

input to the plasma, which is the sum of the dissipative joule heating and the reversible Lorentz work. In the absence of the Hall effect ($b_\infty = 0$) the transverse Lorentz force is zero, and the boundary layer becomes two-dimensional.

Modified Boundary-Layer Equations

It is convenient to modify the axial-momentum equation by noting the invariance of dp/dx across the boundary layer. Thus, $dp/dx = j_\infty B - \rho_\infty u_\infty du_\infty/dx$, and Eq. (14) may be written as

$$\rho \left(u \frac{\partial u}{\partial x} + w \frac{\partial u}{\partial z} \right) = \rho_\infty u_\infty \frac{du_\infty}{dx} + \frac{\partial}{\partial z} \left(\mu \frac{\partial u}{\partial z} \right) + B(j_y - j_\infty) \quad (17)$$

The last term on the right-hand side shows the effect of the variation of the current density across the boundary layer. If the current density in the boundary layer is larger than that in the freestream, the effect is to thin the velocity boundary layer, as does a favorable pressure gradient. Conversely, a smaller current density in the boundary layer has an effect analogous to that of an adverse pressure gradient. Similarly, we can eliminate E_y from Eq. (16) by noting that $j_\infty E_y = \rho_\infty u_\infty dH_\infty/dx$, so that

$$\rho \left(u \frac{\partial H}{\partial x} + w \frac{\partial H}{\partial z} \right) = \frac{1}{Pr} \frac{\partial}{\partial z} \left(\mu \frac{\partial H}{\partial z} \right) + \left(1 - \frac{1}{Pr} \right) \frac{\partial}{\partial z} \left[\mu \frac{\partial}{\partial z} \left(\frac{u^2 + v^2}{2} \right) \right] + j_x E_x + \rho_\infty u_\infty \frac{j_y}{j_\infty} \frac{dH_\infty}{dx} \quad (18)$$

Transformation of Boundary-Layer Equations

Let us now consider the reduction of Eqs. (13–16) to ordinary differential equations. The transformation to be used is that originally employed by Stewartson, modified by Levy,⁷ and further modified by Kerrebrock¹ for a freestream flow of constant temperature. This transformation requires that x and z be replaced respectively, by

$$\bar{x} = \int_{x_0}^x \frac{\rho}{\rho_0} \frac{u_\infty}{u_0} dx \quad (19)$$

and

$$\eta = (u_0/2\nu\bar{x})^{1/2} \bar{z} \quad (20)$$

where

$$\bar{z} = \frac{u_\infty}{u_0} \int_0^z \frac{\rho}{\rho_0} dz \quad (21)$$

The subscript 0 denotes a reference point in the freestream other than the origin, since the pressure is singular there. In this paper the reference point will normally be the channel entrance.

The dependent variables are nondimensionalized by the following relationships:

$$u/u_\infty = f'(\bar{x}, \eta) \quad v/u_\infty = r(\bar{x}, \eta)$$

where the prime denotes differentiation with respect to η , and

$$T_g/T_{g\infty} = \theta(\bar{x}, \eta) \quad (H - H_w)/(H_\infty - H_w) = g(\bar{x}, \eta)$$

Defining the stream function ψ in the usual way so that

$$\frac{\partial \psi}{\partial z} = \frac{\rho}{\rho_0} u \quad \frac{\partial \psi}{\partial x} = -\frac{\rho}{\rho_0} w$$

we find that

$$\psi = (2u_\infty\nu_0)^{1/2} \bar{x}^{1/2} f$$

With this transformation, the boundary-layer equations become the following:

Axial Momentum

$$f''' + ff'' + 2\bar{x} \left[f' \frac{\partial f'}{\partial \bar{x}} - f'' \frac{\partial f}{\partial \bar{x}} \right] + \frac{2\bar{x}}{u_\infty} \frac{du_\infty}{d\bar{x}} \left[\theta - (f') + \frac{\theta}{K} \left(\frac{j_y}{j_\infty} - 1 \right) \right] = 0 \quad (22)$$

Transverse Momentum

$$r'' + fr' - 2\bar{x} \left[f' \frac{\partial r}{\partial \bar{x}} - r' \frac{\partial f}{\partial \bar{x}} \right] - \frac{2\bar{x}}{u_\infty} \frac{du_\infty}{d\bar{x}} \left[rf' + \frac{\theta}{K} \frac{j_x}{j_\infty} \right] = 0 \quad (23)$$

Energy

$$\frac{1}{Pr} g'' + fg' - 2\bar{x} \left[f' \frac{\partial g}{\partial \bar{x}} - g' \frac{\partial f}{\partial \bar{x}} \right] + \left(1 - \frac{1}{Pr} \right) \frac{(\gamma - 1)M_\infty^2}{1 - \theta_w + [(\gamma - 1)/2]M_\infty^2} [f'f''' + (f'')^2 + rr'' + (r')^2] - \left(\frac{2\bar{x}}{u_\infty} \frac{du_\infty}{d\bar{x}} \right) \frac{(\gamma - 1)M_\infty^2}{1 - \theta_w + [(\gamma - 1)/2]M_\infty^2} \times \left[f'g - \theta \left(\frac{j_y}{j_\infty} - b_\infty \left(\frac{K - 1}{K} \right) \frac{j_x}{j_\infty} \right) \right] = 0 \quad (24)$$

It has been assumed that the freestream temperature is constant, and the one-dimensional flow relation $j_\infty E_y = \rho_\infty u_\infty dH_\infty/dx$ has been used to simplify the coefficients

The temperature ratio θ is related to the principal dependent variables through the definitions of H and g :

$$\theta = \theta_w + g(1 - \theta_w) + [(\gamma - 1)/2]M_\infty^2[g - (f')^2 - r^2] \quad (25)$$

The four foregoing equations and the equations for the ratios of current density, electrical conductivity, and Hall parameter to their freestream values describe the flow in the insulator boundary layers

The boundary conditions at the wall ($\eta = 0$) are $f = 0$ and $f' = r = g = 0$. At the edge of the boundary layer ($\eta = \infty$), $f' = g = 1$ and $r = 0$

Conditions for Similar Solutions

Similar solutions will exist if the complete set of the boundary-layer equations and their boundary conditions are independent of \bar{x} . The explicit partial differentiations with respect to \bar{x} appearing in the momentum and energy equations will be equal to zero if the remaining terms in each equation are independent of \bar{x} . This requires that the following conditions be met:

1) θ_w is constant. For a constant freestream temperature, this implies constancy of T_{gw} , which is a reasonable engineering condition for the most efficient use of wall materials

2) The freestream Hall parameter b_∞ is constant. This will be assumed, and the validity of the approximation will be discussed in the next section

3) The electromagnetic loading factor K is constant

4) The term $(2\bar{x}/u_\infty)(du_\infty/d\bar{x})$ is constant

These conditions are necessary but not sufficient for exact similarity, since the freestream Mach number, which is a function of x and thus \bar{x} , appears in the equation for θ and in the energy equation. Exact similarity will exist only if one of the following additional conditions is met:

5) The freestream Mach number M_∞ is zero. This condition is of trivial interest for an MHD device, particularly an accelerator

6) The term $[g - (f')^2 - r^2]$ is inversely proportional to the freestream Mach number M_∞ and $M_\infty^2 \gg (1 - \theta_w)$

Numerical solutions show that the first of these conditions is not met for the model used in this analysis

Assuming that conditions 3 and 4 can be met by an appropriate choice of a freestream velocity, we see that exact similarity exists only for the case when M_∞ is equal to zero. As M_∞ increases, the coefficients in the energy equation which contain M_∞^2 increase until $M_\infty^2 \gg (1 - \theta_w)$, after which they are constant. The term involving Mach number in the expression for θ [Eq. (25)], however, increases without limit, and, therefore, there is not exact similarity at large freestream Mach numbers

If the freestream Mach number varies slowly with \bar{x} , the approximation of local similarity may be useful, since then the terms involving $\partial f/\partial \bar{x}$, $\partial f'/\partial \bar{x}$, $\partial r/\partial \bar{x}$, and $\partial g/\partial \bar{x}$ may be expected to be small

Local similarity will be assumed in this analysis. The validity of the approximation will be discussed in a subsequent section. In the next section, a special class of freestream flows will be determined that satisfies condition 3 exactly and condition 4 approximately

Freestream Flow

In order to obtain similar solutions in boundary-layer problems, it is usually necessary to constrain certain properties of the freestream flow. In Ref. 1, it was demonstrated that the classical "wedge flow" solution of Falkner and Skan yields similar solutions at low Mach numbers for the electrode boundary layer. Unfortunately, for the insulator boundary layers this flow does not satisfy the requirement for a constant, freestream, electromagnetic loading. Culick,⁹ using the approach of Li and Nagamatsu,¹⁰ was unable to find a class of similar solutions for the insulator boundary layer. He did mention the possibility of a singular flow, and, in fact, it is such a flow that will be used in this analysis.

In the channel flow approximation, the equations governing the freestream flow with constant temperature are as follows:

Continuity

$$\rho_\infty u_\infty A = \dot{m} = \text{const} \quad (26)$$

Energy

$$dp/dx = -(j_\infty^2/u_\infty \sigma_\infty) \quad (27)$$

Total Energy

$$p_\infty u_\infty^2 (du_\infty/dx) = j_\infty E_y \quad (28)$$

where j_∞ is given by Eq. (3) and $p = \rho_\infty RT_\infty$

With the definition of the loading parameter given previously, we may write $E_y = (K/K - 1) j_\infty / \sigma_\infty$. Eliminating ρ_∞ from Eq. (28) with the equation of state, we can write the equation for the total energy as

$$p = RT_{g0} [K/(K - 1)] \zeta$$

where $\zeta = j_\infty^2 / \sigma_\infty u_\infty^2 (du_\infty/dx)$

Differentiating this expression for p and equating the result to dp/dx from Eq. (27) results in a differential equation for ζ , which, when integrated, yields

$$\zeta = \zeta_0 \exp \left\{ -\frac{\gamma M_0^2}{2} \left(\frac{K - 1}{K} \right) \left[\left(\frac{u_\infty}{u_0} \right)^2 - 1 \right] \right\} \quad (29)$$

Here ζ_0 , M_0 , and u_0 are reference values of these variables. They will be taken as equal to the reference variables for the similarity transformation of the preceding section and hence will denote the variables at the channel entrance

If the freestream velocity is chosen to be of the form

$$\frac{u_\infty}{u_0} = \left[1 + \frac{2}{M_0^2} \left(\frac{K}{K - 1} \right) \ln \frac{x}{x_0} \right]^{1/2} \quad (30)$$

then Eq. (29) becomes $\zeta = \zeta_0(x_0/x)$, where x_0 is the coordinate

of the channel entrance. Thus a solution does exist for the freestream equations for a constant temperature and a constant electromagnetic loading. Note that this solution does not specifically require σ_∞ to be constant, although the constant temperature and the decrease of pressure and freestream current as the flow moves downstream tend to keep σ_∞ approximately constant.

Computing the coefficient $(2\bar{x}/u_\infty)(du_\infty/d\bar{x})$ from these results, we find

$$\frac{2\bar{x}}{u_\infty} \frac{du_\infty}{d\bar{x}} = \frac{2}{3} \left[1 - \left(\frac{M_0}{M_\infty} \right)^3 \right] \quad (31)$$

where M_0/M_∞ is identical with u_0/u_∞ . Equation (31), in conjunction with the boundary-layer equations (22-24), shows that the electromagnetic fields have little influence in the initial growth of the boundary layers. Physically, this is due to the thinness of the boundary layers and the large acceleration of the flow in this region. It will be assumed that $(M_0/M_\infty)^3 \ll 1$, so that

$$(2\bar{x}/u_\infty)(du_\infty/d\bar{x}) = \frac{2}{3} \quad (32)$$

The analysis then does not apply to the region near the channel entrance, in which the boundary-layer growth is dominated by viscous effects.

Freestream Variables

It is now possible to write expressions for the freestream variables. The characteristics of the flow can more easily be seen by inverting Eq. (30); then the channel length $L = x - x_0$ required to give a specified M_∞ is

$$L = x_0 \left[\exp \left\{ \frac{\gamma}{2} \left(\frac{K-1}{K} \right) (M_\infty^2 - M_0^2) \right\} - 1 \right] \quad (33)$$

where

$$x_0 = \frac{p_0}{\sigma_0 u_0 B_0^2 (K-1)^2} = \frac{\dot{m}}{\gamma M_0^2 A_0 \sigma_0 B_0^2 (K-1)^2}$$

x_0 is descriptive of the configuration and freestream performance of the accelerator; the smaller the x_0 , the shorter the channel length required and thus the greater the acceleration. The quantity x_0 is decreased by increasing the electromagnetic loading K , the entry velocity u_0 , the electrical conductivity, and the magnetic field or by decreasing the pressure.

For a given channel configuration and given gas properties, the exponential term in Eq. (33) shows that the largest acceleration occurs in the region of the channel entrance and decreases with increasing M_∞ . This can also be seen by differentiating Eq. (30) with respect to x and expressing it in the form

$$\frac{dM_\infty}{dx} = \left(\frac{K}{K-1} \right) \frac{1}{\gamma M_\infty x}$$

The freestream electromagnetic loading factor K is an important design parameter for an electromagnetic accelerator. Physically, it represents the ratio of the total input power to the rate of Lorentz work. Thus, the reciprocal of K is descriptive of the electromagnetic conversion efficiency of the accelerator. As K approaches unity, the efficiency approaches unity, but the input power approaches zero, and the channel length becomes infinite. Although, in principle, K can be large, a practical limit appears to be in the neighborhood of $K = 2$, where the joule heating and Lorentz work are equal. The probable range of interest for an accelerator is $1 < K < 2$.

The freestream current density can be expressed as

$$\frac{j_\infty}{j_0} = \left(\frac{\sigma_\infty}{\sigma_0} \right)^{1/2} \left(\frac{M_\infty}{M_0} \right)^{1/2} \exp \left\{ -\frac{\gamma}{2} \left(\frac{K-1}{K} \right) (M_\infty^2 - M_0^2) \right\} \quad (34)$$

The required transverse electric field is

$$\frac{E_y}{E_{y0}} = \left(\frac{\sigma_0}{\sigma_\infty} \right)^{1/2} \left(\frac{M_\infty}{M_0} \right)^{1/2} \exp \left\{ -\frac{\gamma}{2} \left(\frac{K-1}{K} \right) (M_\infty^2 - M_0^2) \right\} \quad (35)$$

and the input power density becomes

$$\frac{j_\infty E_y}{j_0 E_{y0}} = \frac{M_\infty}{M_0} \exp \left\{ -\gamma \left(\frac{K-1}{K} \right) (M_\infty^2 - M_0^2) \right\} \quad (36)$$

The prescribed magnetic field is determined from Eq. (35) and the relation $K = E_y/u_\infty B$ to be

$$\frac{B}{B_0} = \left(\frac{\sigma_0}{\sigma_\infty} \right)^{1/2} \left(\frac{M_0}{M_\infty} \right)^{1/2} \exp \left\{ -\frac{\gamma}{2} \left(\frac{K-1}{K} \right) (M_\infty^2 - M_0^2) \right\} \quad (37)$$

The cross-sectional flow area may be computed from the continuity equation and the equation of state as

$$\frac{A}{A_0} = \frac{M_0}{M_\infty} \exp \left\{ \frac{\gamma}{2} \left(\frac{K-1}{K} \right) (M_\infty^2 - M_0^2) \right\} \quad (38)$$

Strictly, the variation of the freestream Hall parameter can be determined from the appropriate freestream relations; however, we shall treat it as an independent parameter.

Solution of Equations

With the approximations of local similarity and $(M_0/M_\infty)^3 \ll 1$, the system of partial differential equations is reduced to a set of ordinary differential equations with the one independent variable η . The equations can now be written as follows:

Axial Momentum

$$f''' = -ff'' - \frac{2}{3} \left[\theta - (f')^2 + \frac{\theta}{K} \left(\frac{j_y}{j_\infty} - 1 \right) \right] \quad (39)$$

Transverse Momentum

$$r'' = -fr' + \frac{2}{3} \left[rf' + \frac{\theta}{K} \frac{j_x}{j_\infty} \right] \quad (40)$$

Energy

$$g'' = Pr \left\{ -fg' - \left(1 - \frac{1}{Pr} \right) \frac{(\gamma-1)M_\infty^2}{1-\theta_\infty + [(\gamma-1)/2]M_\infty^2} \times \right. \\ \left. [f'f''' + (f'')^2 + rr'' + (r')^2] + \frac{2}{3} \times \right. \\ \left. \frac{(\gamma-1)M_\infty^2}{1-\theta_\infty + [(\gamma-1)/2]M_\infty^2} \left[f'g - \theta \left\{ \frac{j_y}{j_\infty} - b_\infty \times \right. \right. \right. \right. \\ \left. \left. \left. \left(\frac{K-1}{K} \right) \frac{j_x}{j_\infty} \right\} \right] \right\} \quad (41)$$

Also required for the solution of these equations are Eq. (25) for θ , Eq. (7) or (10) for σ/σ_∞ , Eqs. (4) and (5) for j_x/j_∞ and j_y/j_∞ , and Eq. (11) or (12) for b/b_∞ .

Two plasma conditions are considered: thermal equilibrium and thermal nonequilibrium. For the equilibrium case, Eqs. (7) and (11) apply, γ is assigned a value of $\frac{4}{3}$ corresponding to a polyatomic gas, and λ is assigned a value of 7.5 corresponding to cesium at 3000°K. For the nonequilibrium case, Eqs. (10) and (12) apply, γ is assigned a value of $\frac{5}{3}$ corresponding to a monatomic gas, Φ is assigned a value of 3 corresponding to argon seeded with potassium at 3000°K, and α is assigned a value of 0.8 corresponding to a large degree of nonequilibrium in such a gas.

The Prandtl number is taken as 0.7 for both thermal equilibrium and nonequilibrium, since it is felt that the degree of ionization is not large enough for the electrons to increase significantly the thermal conductivity of the plasma.¹¹⁻¹³

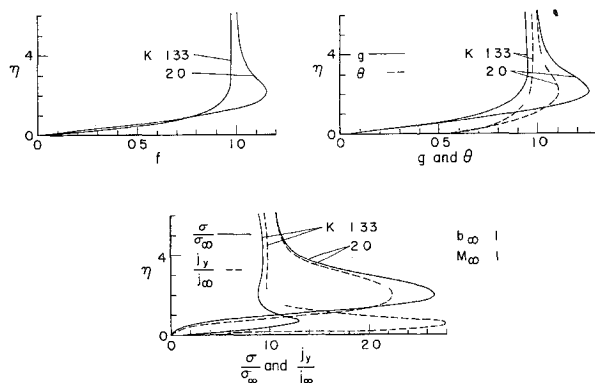


Fig 2 Dependence of the boundary-layer profiles on the electromagnetic loading parameter, $K = E_y/UB$, for nonequilibrium conductivity (f' is the dimensionless velocity, θ and g are the dimensionless temperature and total enthalpy, σ is the electrical conductivity, j_y is the transverse current density, and b_∞ is the freestream Hall coefficient)

The quantity θ_w is assigned the value of 0.5 corresponding to a wall temperature of 1500°K, a reasonable temperature limit for present structural materials. The remaining three parameters, K , M_∞ , and b_∞ , are treated parametrically.

Method of Solution

The system of equations was solved by numerical methods using a forward, step-by-step integration technique on an IBM 7090 computer. The Fortran source program was built around the GLAIDE share program,¹⁴ which uses the Adams four-point method with an auxiliary set of starting equations. The three unknown wall conditions, f_w'' , g_w' , and f_w' , were initially guessed. Using the guessed values, the equations were integrated to the freestream and the next trial values of the wall conditions obtained by a divided differences technique, which is described in Appendix B of Ref 8. This procedure was iterated until satisfactory convergence was obtained at the edge of the boundary layer.

Integration intervals of 0.006, 0.01, 0.02, and 0.05 were initially used. For the remainder of the computations, 0.01 was selected, since it yielded results equal to those for 0.006 within four decimal places. The linear interpolation technique was satisfactory for most values of the parameters. However, for $K = 1.333$, the set of interpolation equations became practically indeterminate as the correct wall values

were approached. As a result, complete convergence at the edge of the boundary layer was not obtained, as can be seen from the profiles in Fig 2. The wall values are believed to be accurate to within $\pm 0.1\%$ for all cases. The accuracy of the profiles varies in accordance with the ease of convergence, but in all cases it is believed to be more than adequate to show the qualitative behavior of the boundary layer.

Results

The principal results of this study are estimates for the coefficients of friction and heat transfer and for the electrical characteristics of the insulator boundary layer. These will be given presently; their significance will be better appreciated if the variations within the boundary layer of velocity, temperature, conductivity, and current density are first examined.

Boundary-Layer Profiles

The boundary-layer profiles for the nonequilibrium plasma are very unusual, largely as a result of the extreme dependence of the conductivity on the magnitude of the electric field measured in coordinates stationary in the flowing gas. The variation of this electric field across the boundary layer is determined by the variation of flow velocity and by the magnitude of K , the electromagnetic loading factor in the freestream. As K is reduced, the acceleration of the freestream and that portion of the energy input to the freestream devoted to joule heating are both decreased, whereas the wall values of the current density and joule heating are increased relative to their freestream values. This can be seen more clearly if we define a local electromagnetic loading factor K_{bl} as $K_{bl} = K/f'$. Since $(K_{bl} - 1)$ is the local ratio of the joule heating to the Lorentz work, the former dominates at any point in the boundary layer where $f' < K/2$. This means that the joule heating will be dominant in the region near the wall and that this region will become thinner as K is reduced.

In discussing the behavior of the nonequilibrium profiles, it will be helpful to have expressions for the gradients of σ and j_y . From Eqs (5) and (10), we find, for $b_\infty = 0$,

$$\frac{d}{d\eta} \log \sigma = \left(\frac{1}{1 - \alpha} \right) \left[\Phi \theta' - \frac{\alpha f''}{K - f'} \right] \quad (42)$$

$$\frac{d}{d\eta} \log j_y = \left(\frac{1}{1 - \alpha} \right) \left[\Phi \theta' - \frac{f''}{K - f'} \right] \quad (43)$$

Thus we see that both σ and j_y can grow or decay exponentially in η , depending on the signs of the bracketed terms. The quantity Φ is taken as 3 in the present work, whereas θ' and f'' would be of the same magnitude for a normal boundary layer (in fact, equal for $Pr = 1$ and a highly cooled wall). Therefore, we should expect very unusual behavior of σ and j_y when $K - f'$ is near $\frac{1}{3}$.

Now let us consider first the effect of variation of the loading parameter K on the boundary-layer profiles for $M_\infty = 1$. We see from Fig 2 that for $K = 2$ there is a large excess of both velocity and temperature, as well as of conductivity and current density. These are consistent, the velocity excess being supported by the excess of current and low density (excess of temperature). The excess of energy in turn is supported by the larger joule heating due to the excess current.

Decreasing K to 1.333 sharpens the concentration of current near the wall, because the ratio of the current density at the wall to its value in the freestream is increased. In addition, the derivatives of σ and j show irregular behavior near the value of η where $K - f' \approx \frac{1}{3}$.

As the Mach number is increased for a constant K of 2, the extreme variations of j_y and σ shown in Fig 3 are found

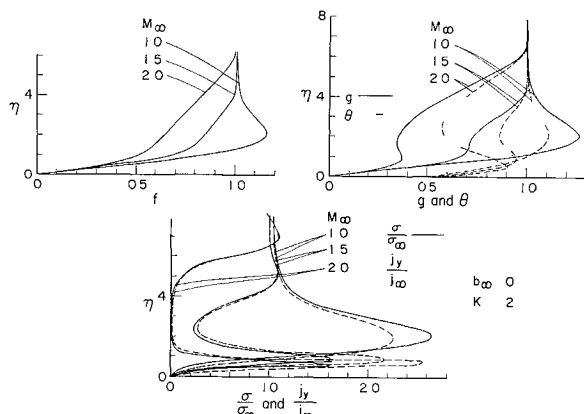


Fig 3 Mach number dependence of boundary-layer profiles for nonequilibrium conductivity (f' is the dimensionless velocity, θ and g are the dimensionless temperature and total enthalpy, σ is the electrical conductivity, j_y is the transverse current density, b_∞ is the freestream Hall coefficient, and $K = E_y/UB$ is the electromagnetic loading parameter)

Table 1 Over-all boundary-layer parameters

Conditions	$\frac{Nu M_0^{1/2}}{\left(\frac{u_0 x_0}{\nu_0}\right)^{1/2}}$	$\frac{C_f \left(\frac{u_0 x_0}{\nu_0}\right)^{1/2}}{M_0^{1/2}}$	$\frac{\delta^*}{\left(\frac{u_0 x_0}{u_0}\right)^{1/2} \left(\frac{x}{x_0}\right) M_0^{1/2}}$
Flat plate	0 33	0 66	1 72
Nonequilibrium $\begin{bmatrix} b_\infty = 0 \\ K = 2 \end{bmatrix}$	3 58	2 62	0 22
Equilibrium $\begin{bmatrix} M_\infty = 1 \end{bmatrix}$	1 84	1 80	0 32
Nonequilibrium			
$M_\infty = 1.5 \begin{bmatrix} b_\infty = 0 \end{bmatrix}$	3 80	1 29	0 48
$M_\infty = 2.0 \begin{bmatrix} K = 2 \end{bmatrix}$	3 92	0 72	0 18
$b_\infty = 1.0 \begin{bmatrix} K = 2 \end{bmatrix}$	3 54	2 58	0 21
$b_\infty = 2.0 \begin{bmatrix} M_\infty = 1 \end{bmatrix}$	3 96	2 80	0 17
$K_\infty = 1.333 \begin{bmatrix} b_\infty = 0 \\ M_\infty = 1 \end{bmatrix}$	5 71	4 52	0 15
Equilibrium			
$M = 2.0 \begin{bmatrix} b_\infty = 0 \\ K = 2 \end{bmatrix}$	2 55	0 67	0 50
Conditions	$\frac{\int_0^\infty (j_y - j_\infty) dz}{j_\infty \left(\frac{\nu_0 x_0}{u_0}\right)^{1/2} \left(\frac{x}{x_0}\right) M_0^{1/2}}$	$\frac{\int_0^\infty j_x dz}{j_\infty \left(\frac{\nu_0 x_0}{u_0}\right)^{1/2} \left(\frac{x}{x_0}\right) M_0^{1/2}}$	$\frac{\int_0^\infty v dz}{u_\infty \left(\frac{\nu_0 x_0}{u_0}\right)^{1/2} \left(\frac{x}{x_0}\right) M_0^{1/2}}$
Flat plate			
Nonequilibrium $\begin{bmatrix} b_\infty = 0 \\ K = 2 \end{bmatrix}$	+2 30		
Equilibrium $\begin{bmatrix} M_\infty = 1 \end{bmatrix}$	-0 95		
Nonequilibrium			
$M_\infty = 1.5 \begin{bmatrix} b_\infty = 0 \end{bmatrix}$	-0 80		
$M_\infty = 2.0 \begin{bmatrix} K = 2 \end{bmatrix}$	-3 05		
$b_\infty = 1.0 \begin{bmatrix} K = 2 \end{bmatrix}$	+2 19	+0 053	-0 010
$b_\infty = 2.0 \begin{bmatrix} M_\infty = 1 \end{bmatrix}$	+2 58	+0 100	-0 018
$K_\infty = 1.333 \begin{bmatrix} b_\infty = 0 \\ M_\infty = 1 \end{bmatrix}$	+0 56		
Equilibrium			
$M = 2.0 \begin{bmatrix} b_\infty = 0 \\ K = 2 \end{bmatrix}$	-0 97		

The current density falls very near to zero over a large part of the boundary-layer thickness for $M_\infty = 2.0$, whereas there is a large excess of current near the wall. The region of low current density is clearly consistent with, and supported by, the corresponding region of low temperature. The region of high current density near the wall results from the increase of effective electric field near the wall, where the velocity is small. It will be noted that there is a narrow region of excess current density near the freestream for $M_\infty = 2$. This is caused by a very small temperature excess that results from viscous heating. Referring again to Eqs (42) and (43), we can correlate the regions of extreme variation of σ and j_y with extremes of f'' and θ' . Of course, these extremes of f'' and θ' are in turn supported by the large variations of body force and joule heating which are associated with the current concentrations and voids.

The effect on the nonequilibrium boundary layer of increasing the Hall parameter b_∞ is shown in Fig 4. The chief over-all effect is to increase the dissipation. The increased joule heating leads to a larger temperature excess, with resultant increases in σ and j_y . The increase in j_y then results in a larger velocity excess.

In detail, the Hall effect is quite complex, as can be seen from the profiles of the axial (Hall) current and transverse velocity. The Hall current actually reverses sign within the boundary layer. It flows in the positive sense in the outer portion of the boundary layer because of the excess of axial velocity there. In the region near the wall, it reverses as the axial velocity becomes small [see Eq (4)]. It is important to note that the Hall current is much smaller than j_∞ everywhere in the boundary layer, even for $b_\infty = 2.0$.

Similarly, the transverse velocities are small. A small flow reversal occurs near the wall for $b_\infty = 1$, but the over-all tendency is for the velocity boundary layer to respond to the average transverse body force.

For the case of equilibrium ionization, the principal question to be answered is whether the depression of conductivity near the wall, by the lowering of the temperature, is sufficient to suppress the short circuiting tendency due to the drop in velocity. It appears from Fig 5 that this is indeed the case, at least up to Mach numbers of 2.

Over-All Boundary-Layer Properties

From these boundary-layer profiles we can derive estimates for several parameters of engineering significance. These are the Nusselt number, coefficient of friction, displacement thickness, and a parameter that measures the excess transverse current in the boundary layer. Estimates for these parameters are tabulated in Table 1. In the upper portion of the table, a standard case, for which $M_\infty = 1$, $K = 2$, $b_\infty = 0$, is compared with the usual high-speed boundary layer on a flat plate. In the lower portions, the variations with each of the parameters are given.

The Nusselt number Nu is defined¹⁵ as $Nu = q_w x / k_w (T_w - T_\infty)$, where q_w , the rate of heat transfer to the wall, is given by $q_w = -k_w (\partial T / \partial z)_w$, and k_w is the coefficient of heat transfer at the wall. In terms of the transformed variables,

$$\frac{Nu}{[(u_0 x_0) / \nu_0]^{1/2} (1 / M_0^{1/2})} = \frac{1}{\theta_w (1 - \theta_w)} \left[\frac{3}{2\gamma M_\infty} \left(\frac{K}{K - 1} \right) \right]^{1/2} \theta_w' \quad (44)$$

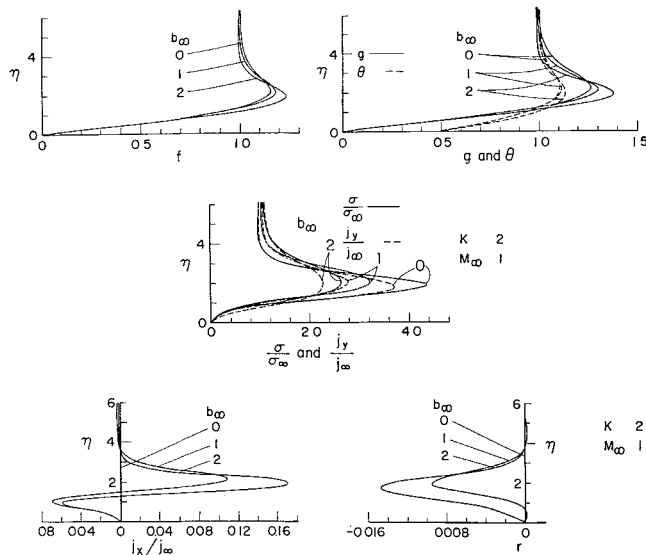


Fig 4 Dependence of the boundary-layer profiles on the freestream Hall coefficient, b_∞ , for nonequilibrium conductivity (f' is the dimensionless velocity, θ and g are the dimensionless temperature and total enthalpy, σ is the electrical conductivity, and j_y is the transverse current density) The bottom figures show the dependence of the three-dimensional boundary-layer profiles on the freestream Hall parameter b_∞ (j_x is the longitudinal Hall current, and r is the transverse dimensionless velocity component)

Thus, there is the normal proportionality between the Nusselt number and the square root of the Reynolds number, with $1/M_0^{1/2}$ representing the variation of the latter with \bar{x} . It must be remembered, however, that the right side of Eq (44) also varies with \bar{x} . For $M_0 = 0.5$, the nonequilibrium $Nu/(u_0 x_0/\nu_0)^{1/2}$ is a factor of 10 larger than that for a comparable nonelectromagnetic boundary layer. It is somewhat smaller for the equilibrium case, but still much larger than for a normal boundary layer. In both cases, it increases with increasing M_∞ . The lower portion of Table 1 shows a slight decrease of the Nusselt number as b_∞ is increased to 1, followed by an increase as b_∞ goes to 2. The largest value of the Nusselt parameter occurs for the non equilibrium case for a K of 1.333.

The axial friction coefficient is defined in the normal manner as $C_f = \tau_x / (\frac{1}{2} \rho_\infty u_\infty^2)$, where $\tau_x = \mu_w u_\infty (\partial f' / \partial z)_w$. After transformation, we find

$$\frac{C_f(u_0 x_0/\nu_0)^{1/2}}{M_0^{1/2}} = \left[\frac{6}{M_\infty^3} \left(\frac{K}{K-1} \right) \right]^{1/2} f_w'' \quad (45)$$

As shown in Table 1, the values are somewhat higher than the usual values for a nonelectromagnetic boundary layer for $M_\infty = 1$ but decrease as M_∞ increases. This is because in the present model the freestream acceleration decreases with increasing M_∞ . The variations with b_∞ and K are similar to those already seen in the Nusselt parameter.

Table 2 Comparison of terms neglected under local similarity assumption^a

η	$2\bar{x} \left(f' \frac{\partial g}{\partial \bar{x}} - g' \frac{\partial f}{\partial \bar{x}} \right)$	$\frac{2}{3} \frac{(\gamma-1)M_\infty^2}{1-\theta_w + [(\gamma-1)/2]M_\infty^2} \times \left(f'g - \theta \frac{j_y}{j_\infty} \right)$
0.6	-0.0487	-2.1096
1.0	-0.3720	-0.2775
2.0	-0.6117	+0.2107

^a For thermal nonequilibrium $b_\infty = 0$, $K = 2$, $M_\infty = 2$

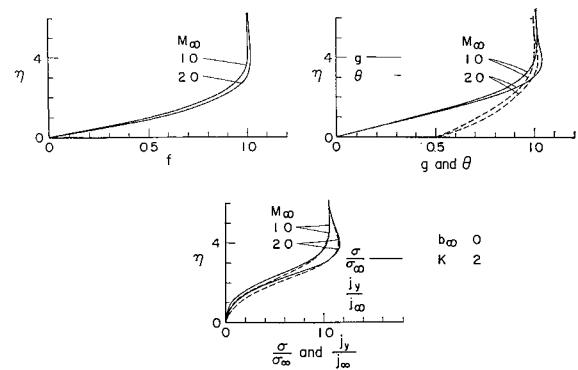


Fig 5 Mach number dependence of boundary-layer profiles for equilibrium conductivity (f' is the dimensionless velocity, θ and g are the dimensionless temperature and total enthalpy, σ and j_y are the conductivity and transverse current, b_∞ is the freestream Hall coefficient, and $K = E_y/UB$ is the electromagnetic loading parameter)

By combining Eqs (44) and (45), a Reynolds' analogy between the heat transfer and the axial skin friction may be developed:

$$\frac{Nu}{C_f(u_0 x_0/\nu_0)(M_\infty/M_0)} = \left[\frac{1}{2\theta_w(1-\theta_w)} \right] \frac{\theta_w'}{f_w''}$$

The usual definition of the displacement thickness is

$$\delta^* = \int_0^\infty \left(1 - \frac{\rho u}{\rho_\infty u_\infty} \right) dz$$

from which, in terms of η ,

$$\frac{\delta^*}{(\nu_0 x_0/u_0)^{1/2}(x/x_0)M_0^{1/2}} = \left[\frac{2}{3} \gamma M_\infty \left(\frac{K-1}{K} \right) \right]^{1/2} \times \int_0^\infty (\theta - f') d\eta \quad (46)$$

From Table 1 it can be seen that, even though the over-all thicknesses of the insulator boundary layers are larger than those for nonelectromagnetic flows, the displacement thickness is less. This is due to the regions of excess velocity.

The magnitude of the average of the excess transverse current in the boundary layer is of interest as a measure of the short circuiting effect on the accelerator. It can be expressed as

$$\frac{\int_0^\infty (j_y - j_\infty) dz}{j_\infty(\nu_0 x_0/u_0)^{1/2}(x/x_0)M_0^{1/2}} = \left[\frac{2}{3} \gamma M_\infty \left(\frac{K-1}{K} \right) \right]^{1/2} \times \int_0^\infty \theta \left(\frac{j_y}{j_\infty} - 1 \right) d\eta \quad (47)$$

For the average of the excess axial (Hall) current, we find

$$\frac{\int_0^\infty j_x dz}{j_\infty(\nu_0 x_0/u_0)^{1/2}(x/x_0)M_0^{1/2}} = \left[\frac{2}{3} \gamma M_\infty \left(\frac{K-1}{K} \right) \right]^{1/2} \times \int_0^\infty \theta \frac{j_x}{j_\infty} d\eta \quad (48)$$

The magnitudes of these average currents do not appear to warrant concern over short-circuiting. It should be noted that the transverse current decreases slightly and then increases as b_∞ is increased to 2, and that the axial current increases with b_∞ as would be expected.

The average of the transverse, or cross flow, velocity in the boundary layer can be determined from the expression

$$\frac{\int_0^\infty v dz}{u_\infty (\nu_0 x_0 / u_0)^{1/2} M_0^{1/2} (x/x_0)} = \left[\frac{2}{3} \gamma M_\infty \left(\frac{K-1}{K} \right) \right]^{1/2} \times \int_0^\infty \theta d\eta \quad (49)$$

As was noted during the discussion of the profiles, it is quite small for the cases considered here

Validity of Principal Assumptions

The assumption of local similarity resulted in the elimination of all terms in Eqs (22-24) containing an explicit variation with \bar{x} . It is now necessary to estimate the effects of neglecting these terms on the numerical results. Since the greatest variations with M_∞ occurred in the enthalpy function g , the neglected terms in Eq (24) were selected for evaluation for the conditions of thermal nonequilibrium, $b_\infty = 0$, $K = 2$, and $M_\infty = 2$. With the neglected terms expressed as

$$2\bar{x} \left(f' \frac{\partial g}{\partial \bar{x}} - g' \frac{\partial f}{\partial \bar{x}} \right) = \frac{2}{3} M_\infty \left(f' \frac{\partial g}{\partial M_\infty} - g' \frac{\partial f}{\partial M_\infty} \right)$$

they can be computed from the results obtained assuming local similarity. In Table 2, the magnitudes are shown at three points in the boundary layer where the greatest changes with M_∞ occur. Also shown are the magnitudes of the last term in Eq (24), which represents the sum of enthalpy flux in the x direction and the input-energy flux. At all three points the neglected terms tend to make g'' more negative, thus accentuating the sharp reduction in the magnitude of the profiles and inhibiting the subsequent return to the free stream values. It appears, therefore, that the terms neglected by the local similarity assumption would not eliminate the unusual behavior of the profiles if they were included.

The neglect of ion-electron collisions and the assumption of slight ionization in developing the expressions for electrical conductivity warrant discussion, in view of the regions of excess temperature and excess current which have been obtained for the case of thermal nonequilibrium. Ion-electron collisions would tend to reduce the magnitude of α , so that the excesses of current density and conductivity are probably overestimated. Similarly, diffusion would tend to reduce the magnitudes of the peaks.

The other major assumption in the nonequilibrium conductivity was that of a constant α and Φ . In fact, α is a function of the gas temperature and approaches unity for large current densities and low gas temperatures. This combination can be seen near the wall as M_∞ is increased (Fig 3). Equation (10) indicates a possibility of instability under these conditions, and thus it appears that the assumption of a constant α may mask potential instabilities in the boundary layer.

Conclusions

In general, it can be concluded that the behavior of the insulator boundary layer can be complex indeed, particularly if nonequilibrium effects couple the gas conductivity to the current density. The effects of compressibility are important at high Mach numbers. Furthermore, the boundary-layer properties are sensitive to relatively small variations of Mach number, Hall parameter, and electromagnetic loading. It appears, therefore, that care must be exercised in the selection of profiles for integral solutions.

For the nonequilibrium case there are large current concentrations that increase the wall shear to three or four

times and the heat transfer to 10 times their values for normal boundary layers. However, the magnitudes of the average current are such that the electrical losses due to shorting do not appear excessive. The results show a marked decrease in the losses with increasing Mach number. The general effect of increasing the Hall parameter is to increase the average current in the boundary layer, leading to thinner boundary layers, increased heat transfer and wall shear, and increased electrical losses. The Hall current and transverse velocity, although increasing with the Hall parameter, are small relative to the freestream current and velocity.

The equilibrium results show that the reduction in conductivity in the boundary layer more than compensates for the excess electric field in the boundary layer and so suppresses the shorting effect. For both types of plasma, the displacement thickness is much less than that for the boundary layer on a flat plate.

The very complicated velocity profiles, with many inflection points, suggest the possibility of hydrodynamic instabilities. In addition, the current concentrations near the wall indicate the possibility of electrical instabilities in the nonequilibrium case. The rapid variation of the profiles with M_∞ casts doubt on the validity of our assumption of local similarity. All of these points require further study. We hope that the present study will suggest possibilities for additional analyses and, perhaps more important, emphasize the need for definitive experiments on insulator boundary layers.

References

- ¹ Kerrebrock, J. L., "Electrode boundary layers in direct current plasma accelerators," *J. Aerospace Sci.* **28**, 631-643 (1961).
- ² Fay, J. A., "Hall effects in a laminar boundary layer of the Hartmann type," *Avco Everett Res. Lab. Res. Rept. 81* (December 1959).
- ³ Moffatt, W. C., "Boundary layer effects in magnetohydrodynamic flows," *Magnetogasdynamics Lab. Rept. 61-4*, Mass Inst. Tech. (May 1961).
- ⁴ Kerrebrock, J. L., "Non equilibrium effects on conductivity and electrode heat transfer in ionized gases," *AFOSR 165 TN 4*, Daniel and Florence Guggenheim Jet Propulsion Center, Calif. Inst. Tech. (November 1960).
- ⁵ Spitzer, L., Jr., *Physics of Fully Ionized Gases* (Interscience Publishers, Inc., New York, 1956), Chap. 2.
- ⁶ Cowling, T. G., *Magnetohydrodynamics* (Interscience Publishers, Inc., New York, 1957), Chap. 6.
- ⁷ Levy, S., "Effect of large temperature changes (including viscous heating) upon laminar boundary layers with variable free stream velocity," *J. Aeronaut. Sci.* **21**, 459-474 (1954).
- ⁸ Reshotko, E. and Beckwith, I. E., "Compressible laminar boundary layer a yawed infinite cylinder with heat transfer and arbitrary Prandtl number," *NACA Rept. 1379* (1958).
- ⁹ Culick, F. E. C., "Magnetogasdynamics channel flow and convective heat transfer," *TN 6*, Daniel and Florence Guggenheim Jet Propulsion Center, Calif. Inst. Tech. (May 1962).
- ¹⁰ Li, T. Y. and Nagamatsu, H. T., "Similar solutions of compressible boundary layer equations," *J. Aeronaut. Sci.* **20**, 653-655 (1953).
- ¹¹ Chapman, S. and Cowling, T. G., *The Mathematical Theory of Non Uniform Gases* (Cambridge University Press, Cambridge, England, 1958), Chap. 18.
- ¹² Jepson, B. M., "Heat transfer in a completely ionized gas," *M.S. Thesis*, Mass Inst. Tech. (1961).
- ¹³ Fay, J. A., "Plasma boundary layers," *AFOSR 994*, Magnetogasdynamics Lab. Rept. 61-8, Mass Inst. Tech. (June 1961).
- ¹⁴ IBM SHARE distribution nos. 413 and 827, GLAIDE 1 (March 14, 1958 and January 11, 1960).
- ¹⁵ Schlichting, H., *Boundary Layer Theory* (McGraw-Hill Book Co., Inc., New York, 1960), p. 298.